CONF-78-148-E
E-0178
EXP. 198
FERMILAB-CONF-78-148-E
RECEIVED
AUG 2 1978
DIRECTORS OFFICE
FERMILAB

PROTON-PROTON ELASTIC SCATTERING FROM 30 TO 250 GeV/c

D. Gross, D. Nitz, S. L. Olsen, G. Warren

University of Rochester, Rochester, New York

K. Abe, R. Bomberowitz, P. Goldhagen, F. Sannes, J. Tortora

Rutgers University, New Brunswick, New Jersey

D. Garbutt, R. Rusack, I. Siotis

Imperial College, London, United Kingdom

ABSTRACT

We present measurements of the proton-proton elastic differential cross section for $1.0 < |t| < 2.0$ $(\mathrm{GeV/c})^2$ for incident proton momenta between 30 and 250 GeV/c. The minimum in the cross section near $t \simeq -1.5$ $(\mathrm{GeV/c})^2$ develops monotonically with increasing incident proton momentum and the cross section remains non-zero up to our highest momentum of 250 GeV/c. The cross section at the second maximum ($t \simeq -1.8$ $(\mathrm{GeV/c})^2$) falls with increasing momentum until 200 GeV/c after which it starts to rise.

Paper submitted to the XIXth International Conference on High Energy Physics, 23-31 August 1978, Tokyo, Japan.

FERMILAB-CONF-78-148-E

In an experiment performed at the Internal Target Area of the Fermi National Accelerator Laboratory we have measured the elastic proton-proton differential cross section for invariant four-momentum transfers squared, $|t|$, between 1.0 and 2.0 $(GeV/c)^2$. Previous measurements[1-5] have indicated that the cross section varies dramatically with energy, particularly at about $t = -1.5$ $(GeV/c)^2$ where a minimum or dip is seen at high energies. In this experiment we measure the development of this structure with energy for incident proton momenta p_o from 30 GeV/c to 250 GeV/c.

The apparatus is shown schematically in Fig. 1. A room temperature hydrogen gas jet was injected vertically across the beam of the main accelerator during the acceleration cycle. Recoil particles from interactions in the jet were detected in a moveable magnetic spectrometer consisting of a superconducting quadrupole doublet and a dipole analyzing magnet. The accelerator vacuum system was extended through and beyond the quadrupoles to a point which corresponded to the horizontal focal point of that system. Thus recoil particles which had the same scattering angle θ_r were focussed to a point at the exit of the vacuum chamber. A Multi-Wire Proportional Chamber, MWPC 1, situated at the vacuum exit registered this position and thus enabled the inference of the scattering angle θ_r to a precision of ±0.1 mr with essentially no error introduced due to multiple scattering.

The momentum p_r of the recoil particle was determined by measuring the bending angle through the dipole using coordinates determined by MWPC's 2 through 5. The precision of this measurement was limited by multiple scattering in MWPC's 3 and 4 which were situated on either side of the analyzing magnet. These chambers were manufactured with 6 micron Acclar windows and were immersed in a helium bag which extended from

MWPC 2 to 5. The uncertainty in the momentum measurement was found to be $\Delta p_r \simeq \pm 0.001$ GeV/c.

A moveable hodoscope consisting of three rows of twenty 7 mm × 7 mm scintillators was placed 25 m downstream from the target to detect the forward proton. These counters were overlapped so that protons originating in the gas jet registered in at least two hodoscope elements. A flared section of beam pipe was installed with a o.5 mm stainless steel window to reduce the amount of material between the target and the hodoscope.

Two stacks of solid state detectors were situated in a separate extension of the accelerator vacuum system at 85° from the beam direction. These detectors measured proton-proton elastic scattering at $t = -0.05$ $(\text{GeV/c})^2$ and were used to monitor the beam-gas jet luminosity in a manner analogous to that described in Reference 6.

The incident momentum was selected by varying the time at which the jet was pulsed relative to the start of the accelerator cycle. Since the recoil kinematics for elastic scattering changes only slowly with the incident momentum over the range covered in this experiment, detection and analysis efficiencies for the recoil spectrometer at any t setting were independent of the incident momentum. Thus the low energy data, where the elastic signals were clear and unambiguous, could be used to determine these quantities.

At the high energies the primary experimental difficulty was the separation of the elastic process from those inelastic processes $pp \rightarrow pX$ for which M_X, the mass of X, was near the mass of the proton. From the scattering angle and momentum of the recoil proton the mass M_X of the forward system can be inferred from the relation

FERMILAB-CONF-78-148-E

$$M_X^2 = m_p^2 + 2p_o(p_r \cos\theta_r - \frac{\sqrt{p_r^2 + m_p^2} - m_p}{\beta^*}) \ . \qquad (1)$$

Here m_p is the proton mass and β^* is the velocity of the CM system in the laboratory. The experimental resolution in M_X^2, which is dominated by the error in the recoil momentum determination, is proportional to the incident momentum. At $t = -1.5$ GeV/c, $\Delta M_X^2 \simeq \pm 0.0013\ m_p p_o$.

For each event the inferred target position was required to be consistent with the beam-jet interaction region and the tracks before and after the analyzing magnet were required to intersect to within ±1 cm at the dipole magnet midplane. Then a "missing mass" M_X was evaluated from Eq. (1) using the scattering angle θ_r and recoil momentum p_r as determined in the spectrometer. For all t values with $p_o \leqslant 100$ the resulting distributions showed a clear elastic peak at $M_X^2 = m_p^2$ with a continuum of events for $M_X^2 > m_p^2$ corresponding to inelastic processes and no events in the unphysical low M_X^2 region as can be seen in Fig. 2 where a typical mass spectrum is shown. For this range of p_o an elastic signal was extracted by fitting the peak with a Gaussian having a width given by our resolution and a smooth polynomial representing the inelastic background.

For $p_o > 100$ GeV/c we further required that the forward going proton be detected by a proper coincidence in the forward hodoscope. This hodoscope, situated only centimeters from the internal proton beam, had very high instantaneous counting rates. At the higher incicent momenta there were typically 5 hits in coincidence with every spectrometer event. For each event a predicted hit position was inferred from the spectrometer information using an elastic hypothesis. The distances Δ between this

inferred position and the center of each hit element were determined. For those events with $(M_X^2-m_p^2)/p_o < 0.0025\ m_p$ (which included 95% of the elastic events) a clear peak was evident in the Δ distribution centered at $\Delta = 0$ with a width consistent with the experimental resolution; this is the elastic scattering signal, the background under the peak being due to accidental counts. The shape of the background could be determined by using the Δ distribution for those events with $(M_X^2-m_p^2)/p_o > .0025\ m_p$, where essentially all of the events are inelastic. This reproduced the shape of the background quite well and enabled us to extract an elastic signal in an unambiguous way. Figure 3 shows a typical Δ distribution in the dip region for signal (a) and background (b). The background histogram (b) was normalized to the signal histogram (a) in the regions on either side of the elastic peak and the signal remaining after background subtraction is shown in Fig. 3c.

The signals extracted in this way were corrected for detection and analysis efficiencies which were determined from the data itself and also for acceptance as determined from a Monte Carlo calculation. The resulting cross sections are shown in Fig. 4. The uncertainty in the absolute normalization is ±15%. The prominent feature of these data is a minimum or dip at $t \simeq -1.5\ (\mathrm{GeV/c})^2$ which develops monotonically with increasing incident proton momentum. The cross section in the dip is always non-zero up to our highest incident momentum of 250 GeV/c. The bin size in t was choosen to keep the relative statiatical precision roughly uniform from point to point, particularly in the dip region. Different procedures were examined to insure that no structure was hidden by the method used to bin the data.

In Fig. 5a are plotted the cross section in the region of the dip ($1.45 \leqslant |t| \leqslant 1.60$ (GeV/c)^2) vs. the incident momentum. Included for comparison are results from other pp experiments[1-5] and the recent np results of DeHaven et al.[7] Within the quoted errors there is reasonable agreement among the various experiments with the exception of 150 GeV/c where our results are significantly lower than the pp result of ref. 4 and the np results of ref. 7, and 200 GeV/c where we show a cross section somewhat larger than that reported in ref. 3. Figure 5b is a similar plot for the cross section around the second maximum ($1.75 \leqslant |t| \leqslant 2.00$ (GeV/c)^2). The cross section here falls with increasing incident momentum until about p_o = 210 GeV/c, after which it appears to rise with further increases in momentum. This rise with increasing momentum is a general property of elastic scattering models where the eikonal is a function of energy times a function of the impact parameter.[8]

We acknowledge with appreciation the support of Drs. D. Yovanovitch, J. Walker and T. Nash, leaders of the Internal Target Area during the course of our experiment. We also wish to thank sincerely Drs. P. Mantsch, and L. Oleksiuk, as well as Messrs. J. Misek, C. Nila, D. Mizicko and the entire technical staff for their help in setting up and running the experiment. We would also like to acknowledge the contribution of the staffs at our home institutions for their assistance in the construction of the detectors and associated electronics. This work was supported by the Department of Energy and the National Science Foundation, United States, and by the Science Research Council, United Kingdom. One of the authors (SLO) was partially supported by a fellowship from the Alfred P. Sloan Foundation.

FERMILAB-CONF-78-148-E

References

1. A. Bohm et al., Phys. Lett. 49B 491 (1974).

2. N. Kwak et al., Phys. Lett. 58B, 233 (1975).

3. C. W. Akerlof et al., Phys. Lett. 59B, 197 (1975).

4. G. Fidecaro et al., Phys. Lett. 76B, 369 (1978).

5. J. Allaby et al., Nucl. Phys. B52, 316 (1973).

6. Y. Akimov et al., Phys. Rev. D12, 3299 (1975).

7. C. E. DeHaven et al., University of Michigan Preprint HE 78-14 (1978).

8. R. Hanzi, B. Margolis and P. Valin, Phys. Rev. Lett. 32, 1077 (1974).

FERMILAB-CONF-78-148-E

Figure Captions

Fig. 1 Experimental setup inside and adjacent to the Fermilab main ring. The recoil spectrometer angle to the beam can be varied between 33° and 78°. T_{1-4} are scintillation trigger counters, $MWPC_{1-5}$ are Multiwire Proportional Chambers with a total of 14 planes, Q_{1-2} and D are superconducting quadrupole and dipole magnets respectively and $M_{1,2}$ are two stacks of solid state monitor counters.

Fig. 2 Missing mass plot at 100 GeV/c incident momentum and t = -1.84 $(GeV/c)^2$ showing elastic peak and fit to signal and background.

Fig. 3 Distributions of differences between hits in the forward hodoscope and positions predicted from information in the recoil spectrometer. Histogram (a) was generated using missing masses near the proton mass and histogram (b) using masses above the proton mass (see text). The net elastic signal, after normalizing (b) to (a) and subtracting, is shown in histogram (c).

Fig. 4 Differential cross sections for proton-proton elastic scattering.

Fig. 5 The differential cross section a) at the dip ($1.45 \lesssim |t| \lesssim 1.60$ $(GeV/c)^2$) and b) at the secondary maximum ($1.75 \lesssim |t| \lesssim 2.0$ $(GeV/c)^2$). Included are the results of other pp experiments (refs. 1-5), and the np results of DeHaven et al. (ref. 7.).

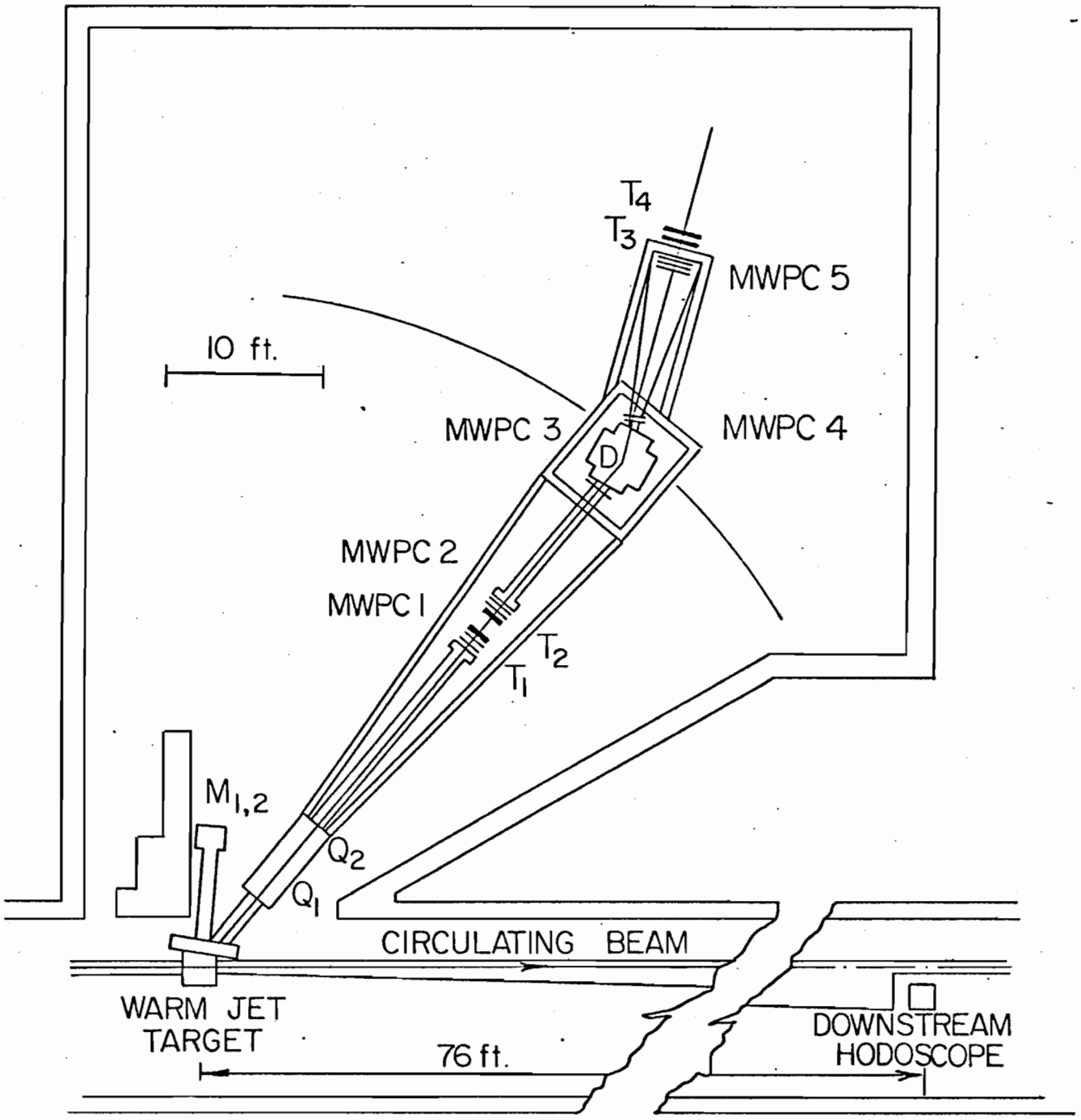
T4
T3
MWPC 5
10 ft.
MWPC 3
MWPC 4
D
MWPC 2
MWPC I
T2
T1
M1,2
Q2
Q1
CIRCULATING BEAM
WARM JET
TARGET
76 ft.
DOWNSTREAM
HODOSCOPE

Fig. 1

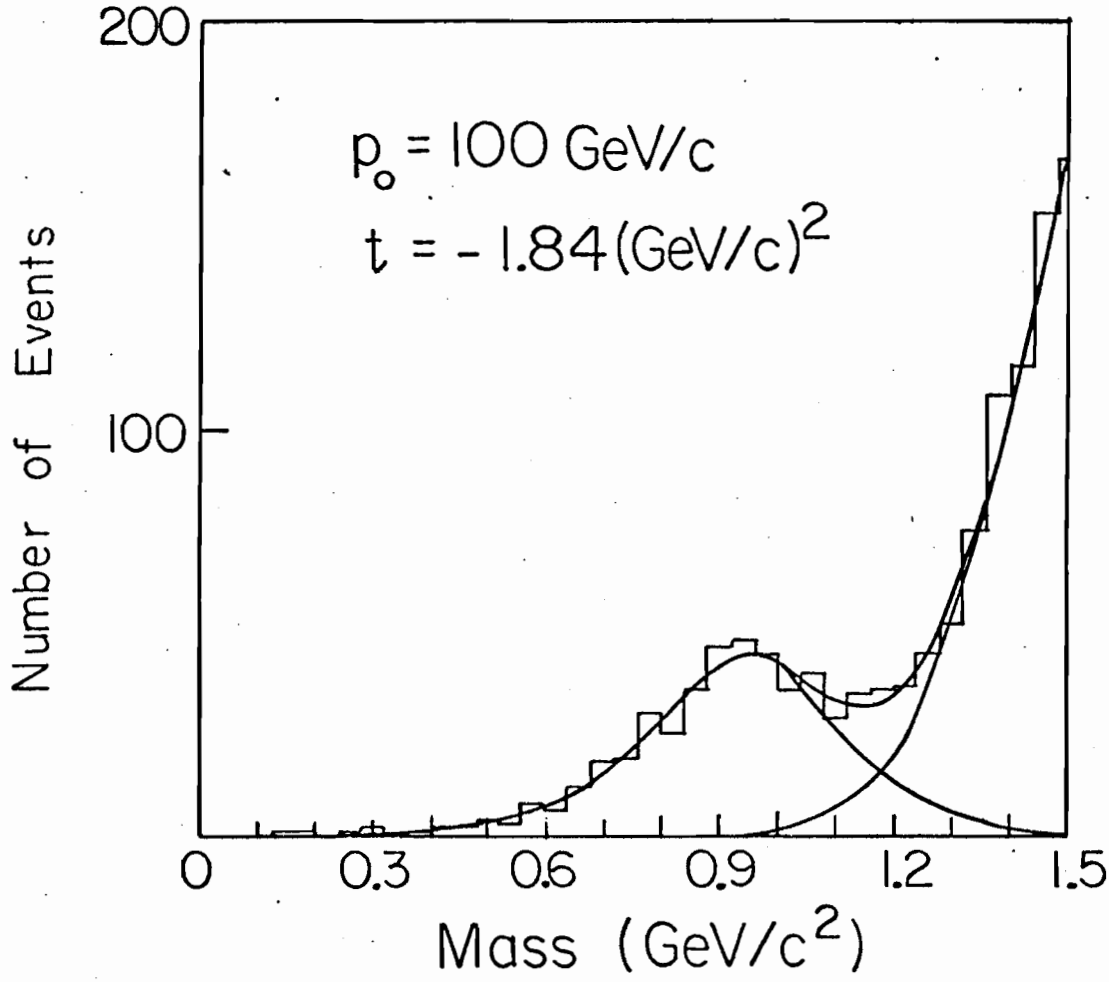
200
100
Number of Events
p_o = 100 GeV/c
t = - 1.84 (GeV/c)^2
0
0.3
0.6
0.9
1.2
1.5
Mass (GeV/c^2)

Fig. 2

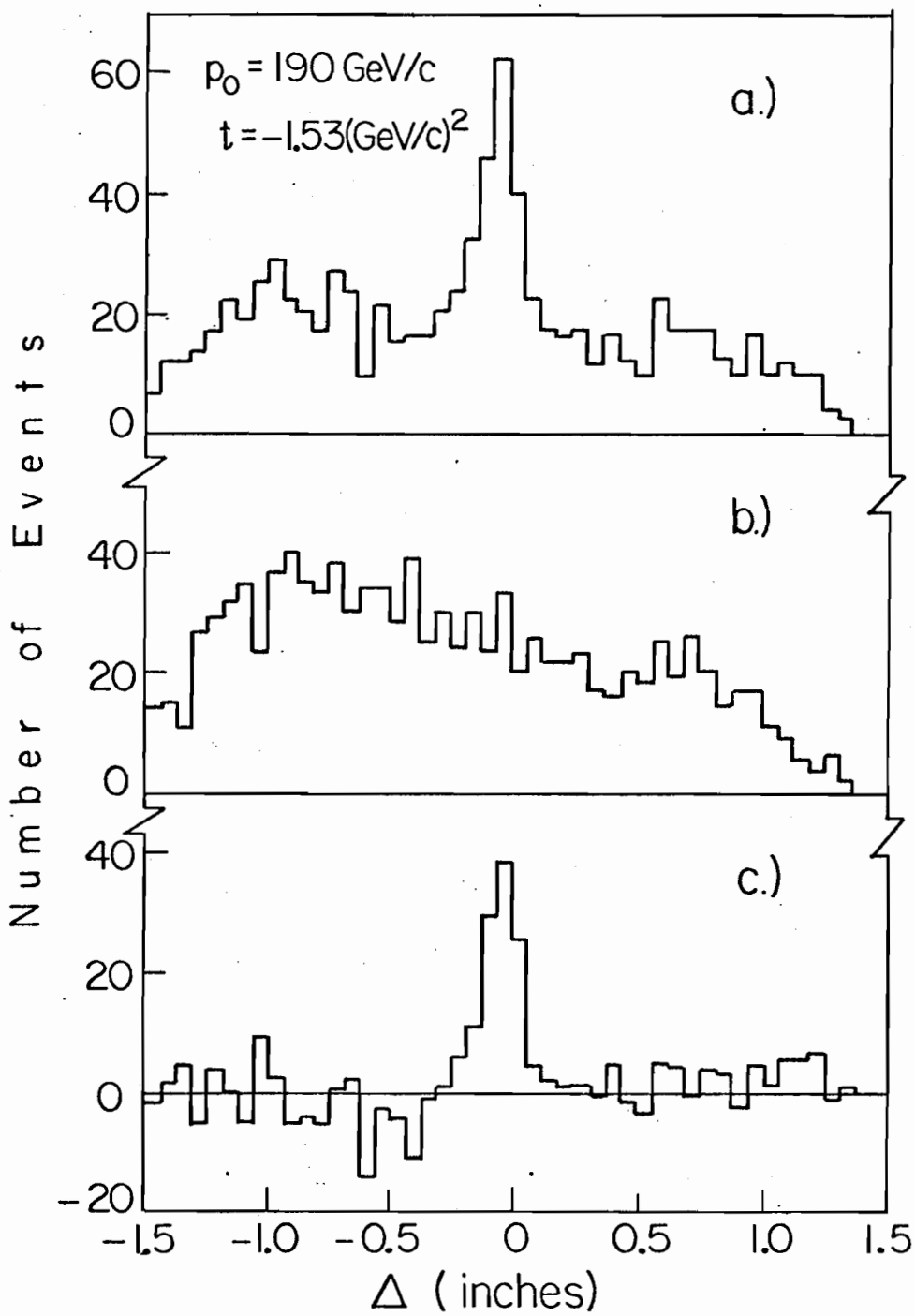
p_0 = 190 GeV/c
t = −1.53(GeV/c)^2
a.)
b.)
c.)
Number of Events
60
40
20
0
40
20
0
40
20
0
−20
−1.5
−1.0
−0.5
0
0.5
1.0
1.5
Δ (inches)

Fig. 3

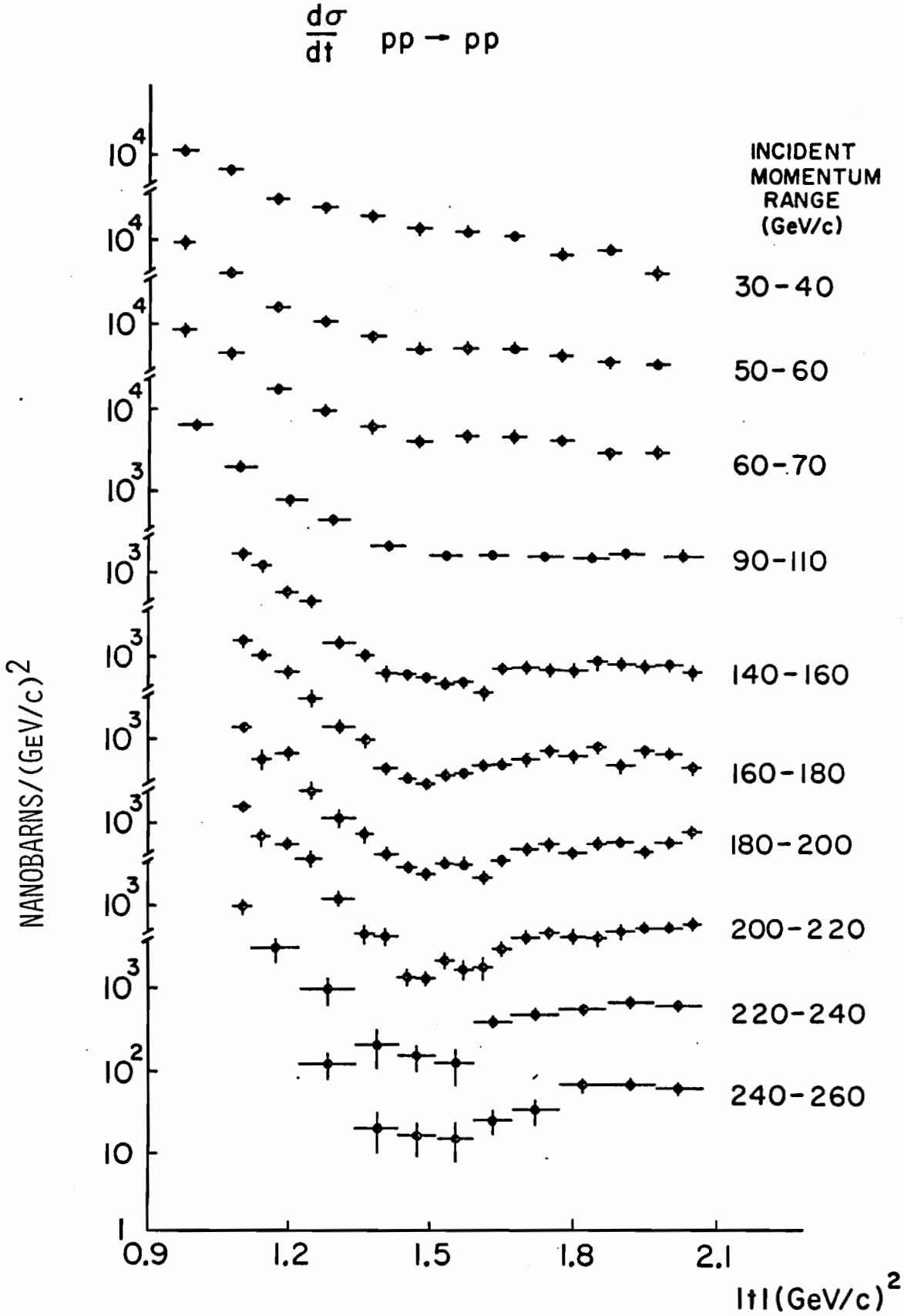
dσ/dt pp → pp
INCIDENT MOMENTUM RANGE (GeV/c)
30-40
50-60
60-70
90-110
140-160
160-180
180-200
200-220
220-240
240-260
NANOBARNS/(GeV/c)²
10⁴
10³
10²
10
1
0.9
1.2
1.5
1.8
2.1
|t|(GeV/c)²

Fig. 4

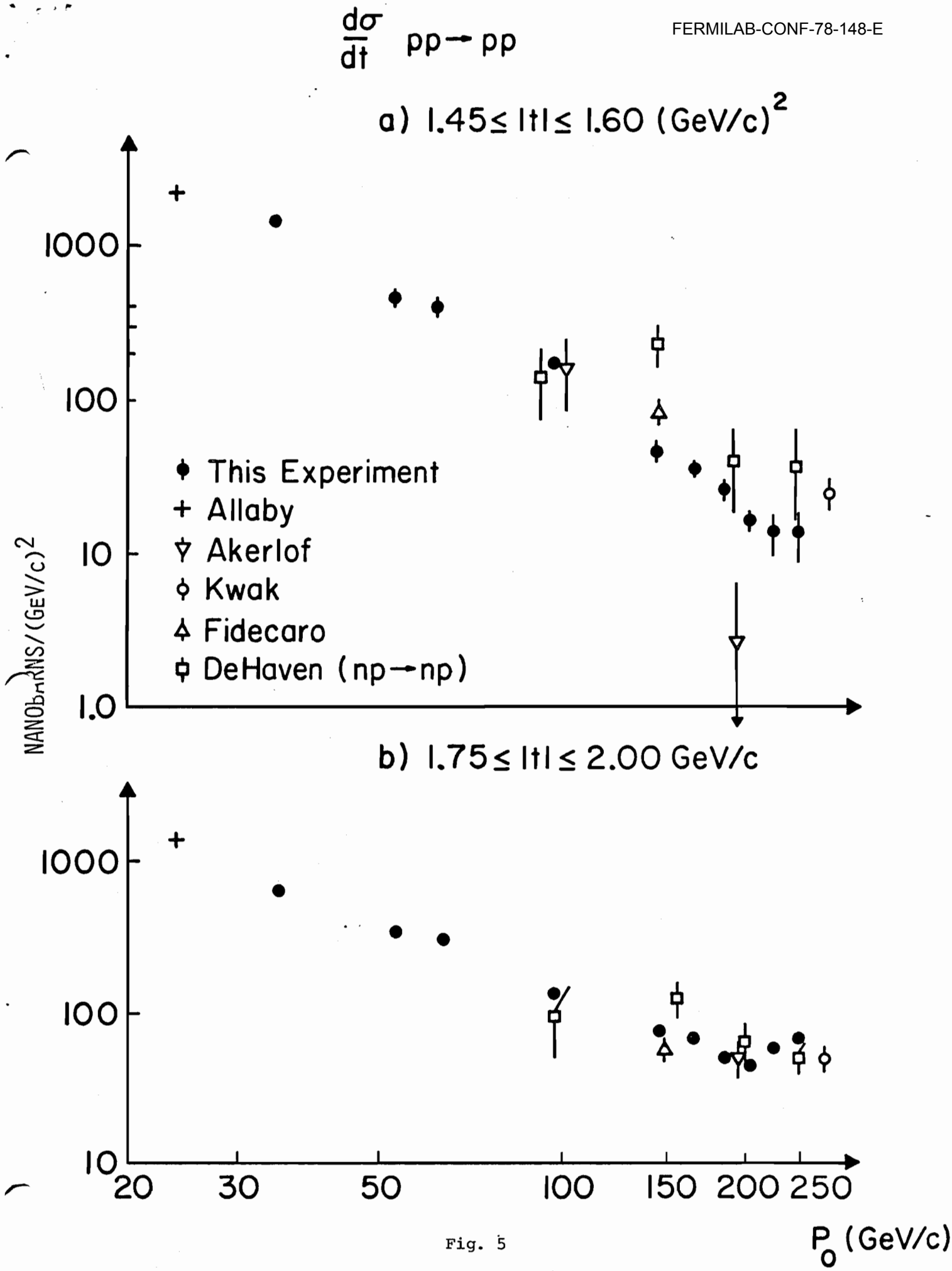
dσ/dt pp→pp
a) 1.45≤ |t|≤ 1.60 (GeV/c)²
1000
100
10
1.0
This Experiment
Allaby
Akerlof
Kwak
Fidecaro
DeHaven (np→np)
NANOBARNS/(GEV/C)²
b) 1.75≤ |t|≤ 2.00 GeV/c
1000
100
10
20
30
50
100
150
200
250
P₀ (GeV/c)

Fig. 5